Aβ-Monomers

DOI: 10.1002/anie.201301537

Distinct Conformational States of the Alzheimer β-Amyloid Peptide Can Be Detected by High-Pressure NMR Spectroscopy**

*Claudia Elisabeth Munte, Markus Beck Erlach, Werner Kremer, Joerg Koehler, and Hans Robert Kalbitzer**

Alzheimer's disease (AD) is one of the most common and severe forms of dementia, but its complex pathogenesis is still not fully understood (for reviews see Refs. [1] and [2]). The typical histological feature of AD is the presence of amyloid plaques in the brains of patients, whose most abundant constituent is the β-amyloid protein (Aβ). According to the widely accepted amyloid hypothesis, Aβ is the primary cause of the disease.[3,4] The Aβ-peptide is produced through proteolytic cleavage of the amyloid precursor protein (APP) by the β- and γ-secretases. The peptide is assumed to have an α-helical conformation as part of APP in the membrane.[5–8] Initially soluble, the peptide assembles into oligomers, which are the primary toxic species,[9,10] and finally forms the fibrils of the amyloid plaques where the peptide has a cross β strand conformation.[11–13]

The polymerization reaction contains two fundamentally different processes, seed formation and elongation of existing fibrils (Figure 1). In both reactions either almost correctly folded monomers (state **1**) or less structured and unstructured monomers (state **2**) could be involved which will interact differently with fibrils (states **3** and **4**) or with small oligomeric seeds (state **5**). For the elongation of stable fibrils (state **4**), the monomers bound in state **3** have to undergo an extensive conformational reorganization. The interaction of the folded conformer **1** (if existing in solution) should have a significant higher affinity to fibrils and different polymerization kinetics compared to the unstructured polymer. It represents a conformation of Aβ possibly important for drug design.

Usually, the peptide is assumed to adopt a predominantly unstructured conformation in solution (state **2**) that only transiently forms helical secondary structure elements.[14–16] Only recently a compact structure of monomeric Aβ was reported.[17] Saturation transfer and ^{15}N relaxation experiments permit the characterization of the reversible interaction of Aβ-monomers with the surface residues of protofibrils (state **1** to state **3** transition), defining direct contact and tethered complexes of the peptides.[18]

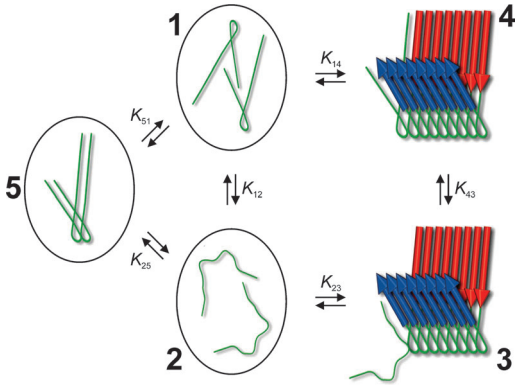

Figure 1. Polymerization of Aβ. The scheme is simplified by the omission of smaller unstable oligomers such as β-balls and different types of fibrils. The analysis of our experimental data shows that state **2** consists of two substates, substate **2′** of partially structured monomers and substate **2″** of purely random-coil-like structures.

The transition of Aβ from a partially α-helical structure of the monomer to a cross β-strand conformation is assumed to be a critical step in pathogenesis of AD[19] but the mechanism of this conversion is still unknown. High-pressure NMR spectroscopy can be used to identify different conformational states of polypeptides that occur under normal pressure in solution through observation of their pressure response. In fact, we can detect a compactly folded state and a partly unfolded state in solution with significantly different molar partial volumes that are coexisting at atmospheric pressure.

A set of ^{1}H,^{15}N HSQC spectra of Aβ(1–40) were recorded at different pressures and temperatures (Figure S1 in the Supporting Information). Most of the amide resonances shift continuously with pressure, the majority of resonances to lower fields. Importantly, the observed pressure-induced chemical shift changes are completely reversible. In order to remove unspecific pressure effects occurring in random-coil structures, the corresponding pressure-dependent shift changes of random-coil model peptides[20] were always subtracted from the experimental data. Thus a random-coil structure would be characterized by vanishing pressure effects. The combined ^{1}H and ^{15}N chemical shift data[21] were fitted with a second-order Taylor expansion [Eq. (1) in the Supporting Information] giving the first- and second-order pressure coefficient B_1* and B_2* (Figure 2). By inspec-

[*] Prof. Dr. C. E. Munte,[+] M. Beck Erlach, Prof. Dr. W. Kremer, J. Koehler, Prof. Dr. H. R. Kalbitzer
Institute of Biophysics and physical Biochemistry
University of Regensburg
Universitätsstrasse 31, 93053 Regensburg (Germany)
E-mail: hans-robert.kalbitzer@biologie.uni-regensburg.de
[+] Present address: Physics Institute of São Carlos
University of São Paulo, São Carlos, SP (Brazil)

[**] This work was supported by the Deutsche Forschungsgemeinschaft (DFG), the Bayerische Forschungsstiftung, the Fonds der chemischen Industrie (FCI), and the Fundação de Amparo à Pesquisa do Estado de São Paulo (FAPESP).

Supporting information for this article (including details on sample preparation, NMR spectroscopy, and the evaluation of the high-pressure data) is available on the WWW under http://dx.doi.org/10.1002/anie.201301537.

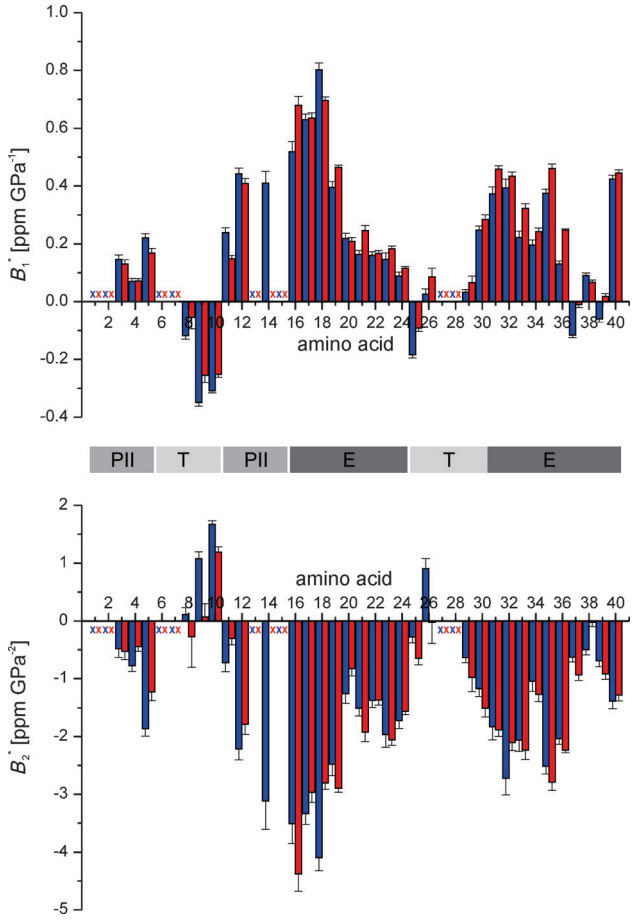

Figure 2. Plot of the first- and second-order pressure coefficients of Aβ(1–40). The sample contained 474 μM ^{15}N-enriched human Aβ(1–40) in 50 mM [D_{11}]Tris, 90 mM NaCl, 50 μM DSS, 0.1 mM dioxane, 1 mM NaN_3, 0.5 mM [D_{16}]EDTA, 8% ^2H_2O, pH 7.0 (DSS = 4,4-dimethyl-4-silapentane-1-sulfonic acid, EDTA = ethylenediaminetetraacetic acid, Tris = tris(hydroxymethyl)aminomethane). The combined first- and second-order pressure coefficients were calculated from the ^{1}H,^{15}N HSQC spectra recorded in pressure steps of 20 MPa up to 200 MPa. Blue: 277 K, red: 288 K, x: residues that could not be detected with sufficient quality. The Taylor coefficients were corrected for random-coil effects (see the Supporting Information). Top: Combined first-order pressure coefficients B_1*. Bottom: Combined second-order pressure coefficients B_2*. Middle: Structural model of Aβ(1–40) in the solution proposed by Danielson et al.[16] PII: propensity for a polyproline II like helix, T: turn or hinge region, E: propensity for an extended strand.

tion of the data one can recognize characteristic clusters of the pressure coefficients in the amino acid sequence that indicate regions that are strongly involved in structural transitions. They correspond to different structural regions proposed for Aβ in the solute and solid state. An example is the region between amino acids 25 to 30 where supposedly a hinge region exists in the solution structures[7,15,16] as well as in the models of fibrillar Aβ.[11–13,22] Structural groups defined by Danielson et al.[16] almost perfectly fit the observed pressure patterns. The two predicted extended regions are characterized by large positive first-order coefficients and negative second-order coefficients. The last residues 37 to 39 have low pressure coefficients, indicative of a more random-coil like structure. The large values of the terminal Val40 could be due to small changes of the protonation state of the carboxyl group with pressure.

When the quality of the pressure-dependent shift changes is high enough, the data can be fitted using a detailed thermodynamic model [Eqs. (2) and (3) in the Supporting Information]. The simplest model assumes two conformational states where the exchange is sufficiently fast to lead to a population-weighted averaging of the chemical shifts of the two states. The pressure-induced chemical shift changes of Aβ can be fitted sufficiently well with this model (Figure 3 a,b). Usually high pressures induce unfolding of polypeptides, in the simplest case random-coil structures are to be expected. Since in Figure 3 also temperature-corrected random-coil shifts[23] were subtracted, at high pressures the deviation of the chemical shifts from the respective random-coil values should approximate zero ppm. With exception of a few residues (e.g. Glu3, Asp23, Met35, Val39) most of the ^{1}H and ^{15}N resonances follow the expected trend and show chemical shift values at high pressure that approach the predicted random-coil values (Figure 3 c,d). However, in most cases the chemical shifts at high pressures do not reach values characteristic for random-coil structures, suggesting that also state **2** is not completely in a random-coil-like conformation. A correlation analysis of the pressure-induced chemical shift changes supports the hypothesis that a correlated process is induced by pressure (Figure S2 in the Supporting Information). A correlated pressure response of the residues from Ser8 to Lys16 and the C-terminal region is observed as it would be the case in a two-state equilibrium. Note that also regions with a correlation coefficient of less than 0.9 show some correlations. Their lower correlation coefficient is mainly due to the quality of the pressure-dependent shift data for these residues. Table 1 summarizes the obtained thermodynamic parameters for the transition from **1** to **2**.

Table 1: Conformational transitions in monomeric Aβ and thermodynamics of polymerization.[a]

T [K]	Transition i–j	K_{ij} (at 0.1 MPa)	ΔG^0_{ij} [kJ mol^{-1}]	ΔV^0_{ij} [mL mol^{-1}]	$\Delta\beta^{0\prime}_{ij}$ [mL MPa^{-1} mol^{-1}]
277	**1**–**2′**	0.48	1.7 ± 0.9	−43.6 ± 1.7	−0.30 ± 0.04
	(**1**,**2′**)–**2″**	0.24	3.3 ± 0.1	−11.8 ± 5.0	0.05 ± 0.03
288	**1**–**2′**	0.42	2.1 ± 0.8	−43.7 ± 1.7	−0.28 ± 0.05
	(**1**,**2′**)–**2″**	0.11	5.2 ± 0.3	−29 ± 13	0.03 ± 0.13

[a] For experimental conditions see Figure 2. The parameters were calculated as described in the Supporting Information. K_{ij}, T, ΔG^0_{ij}, ΔV^0_{ij}, $\Delta\beta^{0\prime}_{ij}$: equilibrium constant $K_{ij} = [j]/[i]$ between states j and i, absolute temperature, difference of partial molar Gibbs energies, partial volumes, and compressibility factors.

The frequency distribution of the obtained thermodynamic parameters is depicted in Figure S3 in the Supporting Information. For an ensemble of polypeptide structures one would expect some variations of the parameters from residue to residue since the observed nuclei may sense different processes that occur simultaneously with the main transition which is described by a two-state model. In fact, such

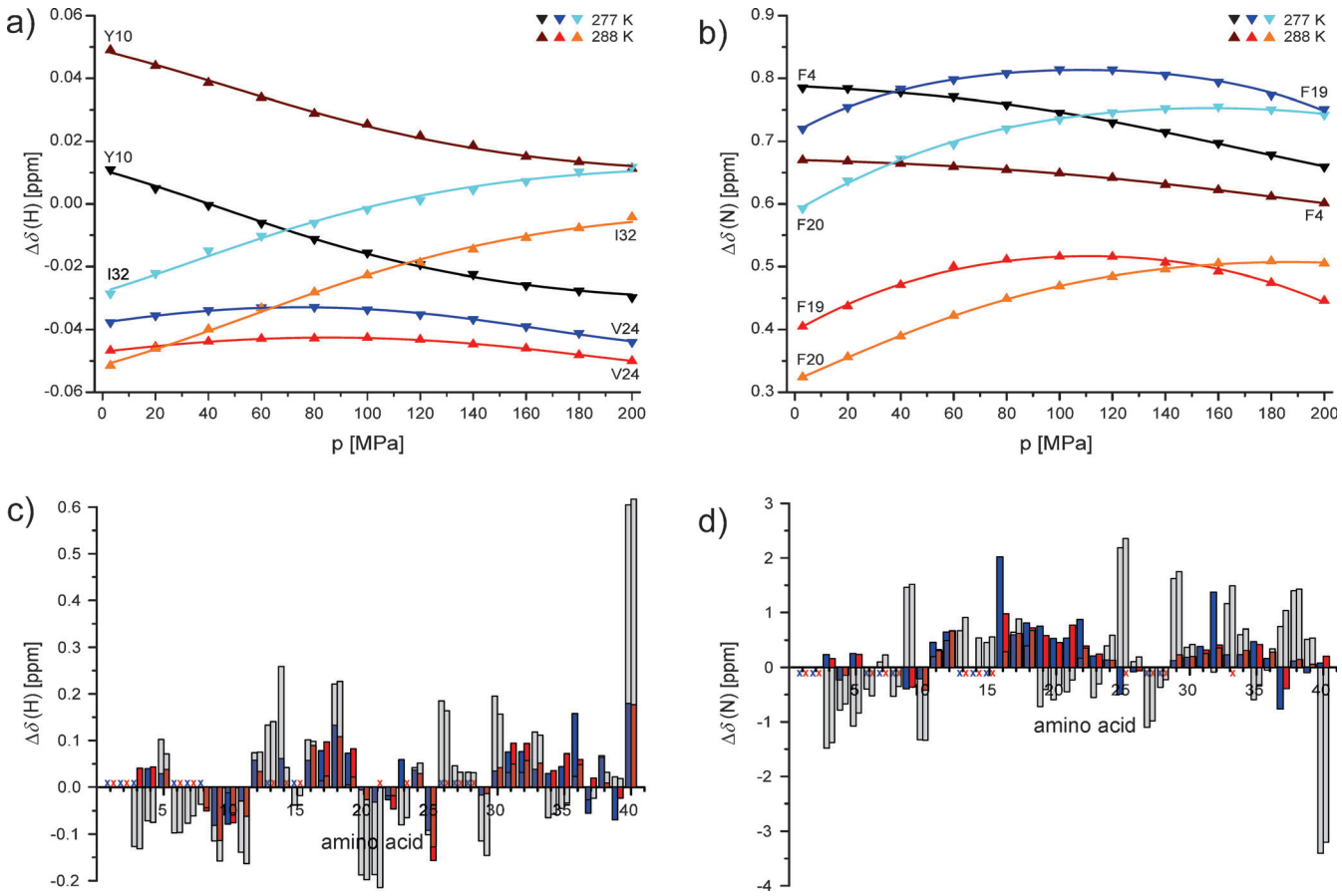

Figure 3. Fit of the pressure-dependent chemical shift changes with a thermodynamic model. The pressure-induced chemical shifts δ of selected residues at 277 and 288 K fitted with Equation (2) are shown (Supporting Information). Before fitting, the data were corrected for the pressure dependence of random-coil shifts.[20] The deviation $\Delta\delta$ from temperature- and pressure-corrected chemical shifts[23] was plotted as function of the pressure for a) ^{1}H chemical shifts, b) ^{15}N chemical shifts. From the fit of the data the chemical shift difference $\Delta\delta_{12}$ between states **1** and **2** is obtained for the amide c) ^{1}H and d) ^{15}N atoms and plotted as a function of the position in the sequence. Blue: 277 K, red: 288 K, x: residues that could not be fitted satisfactorily. In addition the deviation of the chemical shifts at ambient pressure from temperature-corrected random-coil values are depicted as gray bars.

a sequence-specific distribution of the thermodynamic parameters is observed usually in proteins (see for example, the pressure response of the human prion protein reported by Kremer et al.[24]). In addition, the accuracy of the thermodynamic parameters obtained from a fit of the data also strongly depends on the magnitude of chemical shift changes. Thus the observed spread of the parameters is at least partly due to the limited precision of the fit.

Aβ stably incorporated in amyloid fibrils has NMR lines too broad to be observed by solution NMR spectroscopy. In addition to this "dark" state (not visible in solution NMR spectra) Fawzi et al.[18] detected two different binding states of monomeric Aβ to amyloid fibrils, a tethered (*t*) and direct contact (*c*) state corresponding to states **3** and **4** in Figure 1. Increasing the pressure leads to a significant increase of the signal intensities in the ^{1}H NMR spectra, indicating the expected pressure-induced depolymerization as observed earlier for lysozyme amyloid.[25] It is characterized by a generalized strong increase of the backbone and side-chain NMR signals of the monomer (see e.g. Figure S4 in the Supporting Information). In addition to this general increase of the cross peak intensities with pressure, for individual cross peaks in the ^{1}H,^{15}N HSQC spectrum differences in the magnitude of the pressure-induced intensity change can be observed. After a correction of the cross peak volumes for the increase of the monomer concentration with pressure for a number of residues, a pressure-dependent reduction of the cross peak volumes remains (Figure 4). The sequence-specific volume reduction of the amide cross peaks observed here is typical for a slow exchange between (at least) two states (see the Supporting Information). At higher pressures a few weak additional cross peaks can be observed with chemical shifts that are close to typical random-coil positions that may correspond to a substate **2″** of state **2**. Although the magnitude of the observed changes in the amide cross peak volume is also sequence dependent, most of them can be fitted with a similar set of thermodynamic parameters (Figure S5 in the Supporting Information) indicating a common process for the signal reduction. A fit of the pressure dependence of the cross peak volumes [Eq. (10) in the Supporting Information] gives an apparent average partial volume difference of $(-12\pm5)\,\mathrm{mL\,mol^{-1}}$ and $(-29\pm$

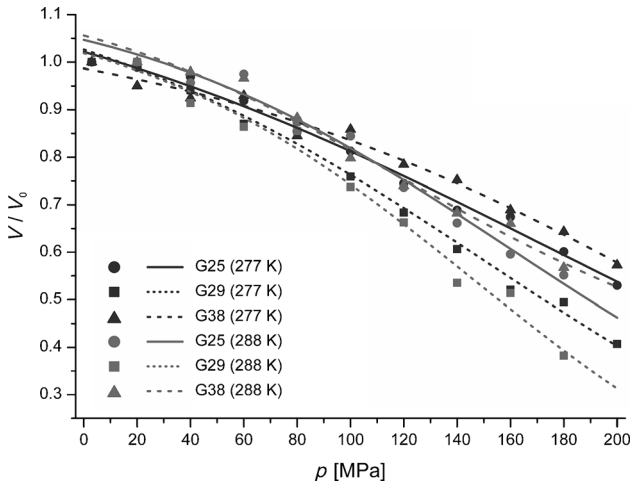

Figure 4. Pressure-dependent volume changes. Example of pressure-induced volume changes $V_i(p)/V_i(p_0)$ of Gly25, Gly29, and Gly38 at 277 K (black) and 288 K (gray) fitted with Equation (5) (see the Supporting Information). Before fitting, the data were corrected for the concentration changes by the pressure-dependent monomerization. For experimental conditions see Figure 2.

13) mL mol^{-1} at 277 K and 288 K, respectively (Table 1). Since in this analysis the transitions from state **1** and state **2′** cannot be separated, the obtained error of ΔV is rather large (Table 1) and only apparent values are obtained from the analysis. The apparent ΔV contains also contributions of the transition between substates **2′** and **2″** where the volume change should be substantially smaller than -12 mL mol^{-1}. From the parameters summarized in Table 1 the relative concentrations of the three states can be calculated for all pressures (Figure 5). At ambient pressure state **1** dominates; about 58 % and 65 % of all molecules in solution are found in folded state **1** at 277 K and 288 K, respectively. In contrast, at intermediate pressures around 100 MPa the partially folded conformation **2′** dominates the equilibrium. At very high

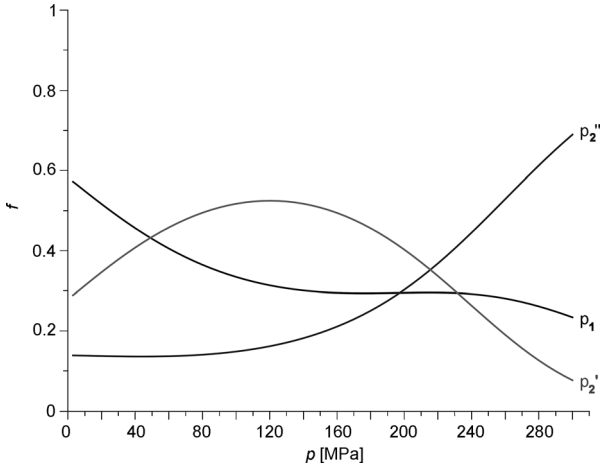

Figure 5. Relative populations of the three conformational states of Aβ. The relative populations *f* of states **1**, **2′**, and **2″** were calculated with the parameters given in Table 1 [Eq. (6) in the Supporting Information] and are plotted as a function of pressure *p* at $T = 277$ K.

pressures the random-coil-like structure **2″** has the highest relative concentration. The partial molar volumes of states **2′** and **2″** are substantially smaller than that of state **1**. Also the compressibility of states **2** and **2′** is significantly smaller than that of the folded state **1** (Table 1). Generally, a decrease of the partial molar volume and the compressibility is characteristic for unfolding processes.

With -43.6 mL mol^{-1} the volume difference between states **1** and **2** is significant, indicating large structural differences. Unfolded structures are characterized by smaller partial volumes; for the denaturation of the well-folded Ras-binding domain of RalGDS (87 residues) we determined a volume change of -78 mL mol^{-1}.[26] This indicates a rather compactly folded structure of Aβ (40 residues) in state **1**. The rather small chemical shift dispersion observed seems to be contradictory to our conclusion. Usually NMR spectroscopists conclude from a small chemical shift dispersion that a protein is unfolded. In most cases this is true since the formation of canonical secondary structures leads to substantially larger chemical shift changes. However, for smaller peptides this is not necessarily true. An example is the inactivation peptide of the potassium channel of Raw3[27] which is compactly folded but does not contain canonical secondary-structure elements and shows a similar chemical shift distribution as Aβ. The chemical shift values deviate significantly from random-coil values (Figure 3) but get closer to the pressure-corrected random-coil values. Also the H^{α} and ^{13}C shifts reported by Hou et al. deviate significantly from random-coil values but allow only the prediction of a short β-strand from V18 to F20 (Figure S6 in the Supporting Information). If state **1** of the Aβ-monomer would have a cross-beta-like structure (a model we would prefer) which is mainly stabilized by side-chain contacts, one would expect a similar chemical shift distribution. A cross-beta structure opening up at higher pressure would also nicely explain the sequential distribution of the pressure coefficients (Figure 2).

NMR parameters such as chemical shifts and NOEs represent only (nonlinear) ensemble averages. In our case we have two structural ensembles with comparable populations. Between states **1** and **2′** the exchange is fast on the NMR time scale. From the maximum chemical shift difference $\Delta\delta$ the exchange correlation time τ_e for the transition between the two states can be estimated as < 1.2 ms. If data are interpreted as corresponding to only one ensemble, incorrect structures can be expected. The calculated structures would depend on the NMR parameters used and the relative populations of the two states that are temperature (this paper) and most probably also pH and ionic strength dependent. Obviously, in most cases these calculations lead to the standard picture of monomeric Aβ that is represented by a random-coil-like structure with transient α-helical contributions.[5–8] At different conditions the compactly folded state **1** may prevail and the nonuniform averaging can produce more compact mean structures like the NMR structure reported by Vivekanandan et al.[17] Surprisingly, only a small population of pure random-coil-like structures exists at ambient pressure (Figure 5, Table 1).

According to our analysis, at ambient pressure the Aβ-monomers occur in two main structural ensembles, a partly

folded or unfolded ensemble **2** and a compactly packed ensemble **1**, which most probably already has structural properties similar to Aβ bound in polymers (Figure 1). If one assumes that the compactly folded state **1** has a higher affinity to existing seeds (β-balls and fibrils), our data explain the temperature and pressure dependence of the polymerization reaction: the population of the high-affinity state **1** increases with temperature in the temperature range studied here and decreases with pressure explaining the observed temperature-induced polymerization and would lead to a pressure-induced depolymerization of Aβ. In the absence of fibrils acting as seeds for the polymerization, the compactly packed state **1** detected here could also contribute to the formation of intermediate states such as β-balls. Stabilization of the partially folded state **2′** (inhibiting the formation of state **1**) by small molecules could also be a suitable mechanism for drug development by weakening the monomer–oligomer interaction similar to the mechanism successfully demonstrated for the interaction of effectors with oncogenic Ras.[28,29]

Received: February 21, 2013
Published online: July 10, 2013

Keywords: Alzheimer's disease · amyloid β-peptides · high-pressure chemistry · NMR spectroscopy

[1] M. P. Mattson, *Nature* **2004**, *430*, 631 – 639.
[2] L. Blennow, M. J. de Leon, H. Zetterberg, *Lancet* **2006**, *368*, 387 – 403.
[3] J. Hardy, D. J. Selkoe, *Science* **2002**, *297*, 353 – 356.
[4] R. E. Tanzi, L. Bertram, *Cell* **2005**, *120*, 545 – 555.
[5] X. P. Xu, D. A. Case, *Biopolymers* **2002**, *65*, 408 – 423.
[6] J. Danielsson, J. Jarvet, P. Damberg, A. Graslund, *Magn. Reson. Chem.* **2002**, *40*, S89 – S97.
[7] O. Crescenzi, S. Tomaselli, R. Guerrini, S. Salvadori, A. M. D'Ursi, P. A. Temussi, D. Picone, *Eur. J. Biochem.* **2002**, *269*, 5642 – 5648.
[8] P. A. Temussi, L. Masino, A. Pastore, *EMBO J.* **2003**, *22*, 355 – 361.
[9] J. P. Cleary, D. M. Walsh, J. J. Hofmeister, G. M. Shankar, M. A. Kuskowski, D. J. Selkoe, K. H. Ashe, *Nat. Neurosci.* **2005**, *8*, 79 – 84.
[10] C. Haass, D. J. Selkoe, *Nat. Rev. Mol. Cell Biol.* **2007**, *8*, 101 – 112.
[11] A. T. Petkova, Y. Ishii, J. J. Balbach, O. N. Antzutkin, R. D. Leapman, F. Delaglio, R. Tycko, *Proc. Natl. Acad. Sci. USA* **2002**, *99*, 16742 – 16747.
[12] T. Lührs, C. Ritter, M. Adrian, D. Riek-Loher, B. Bohrmann, H. Döbeli, D. Schubert, R. Riek, *Proc. Natl. Acad. Sci. USA* **2005**, *102*, 17342 – 17347.
[13] A. T. Petkova, W.-M. Yau, R. Tycko, *Biochemistry* **2006**, *45*, 498 – 512.
[14] R. Riek, P. Güntert, H. Döbeli, B. Wipf, K. Wüthrich, *Eur. J. Biochem.* **2001**, *268*, 5930 – 5936.
[15] L. Hou, et al., *J. Am. Chem. Soc.* **2004**, *126*, 1992 – 2005.
[16] J. Danielsson, A. Andersson, J. Jarvet, A. Graslund, *Magn. Reson. Chem.* **2006**, *44*, S114 – S121.
[17] S. Vivekanandan, J. R. Brender, S. Y. Lee, A. Ramamoorthy, *Biochem. Biophys. Res. Commun.* **2011**, *411*, 312 – 316.
[18] N. L. Fawzi, J. Ying, R. Ghirlando, D. A. Torchia, G. M. Clore, *Nature* **2011**, *480*, 268 – 272.
[19] M. Gross, *Curr. Protein Pept. Sci.* **2000**, *1*, 339 – 347.
[20] J. Koehler, M. Beck Erlach, E. Crusca, Jr., W. Kremer, C. E. Munte, H. R. Kalbitzer, *Materials* **2012**, *5*, 1774 – 1786.
[21] F. H. Schumann, H. Riepl, T. Maurer, W. Gronwald, K.-P. Neidig, H. R. Kalbitzer, *J. Biomol. NMR* **2007**, *39*, 275 – 289.
[22] R. Tycko, *Q. Rev. Biophys.* **2006**, *39*, 1 – 55.
[23] M. Kjaergaard, S. Brander, F. Poulsen, *J. Biomol. NMR* **2011**, *49*, 139 – 149.
[24] W. Kremer, N. Kachel, K. Kuwata, K. Akasaka, H. R. Kalbitzer, *J. Biol. Chem.* **2007**, *282*, 22689 – 22698.
[25] T. N. Niraula, T. Konno, H. Li, H. Yamada, K. Akasaka, H. Tachibana, *Proc. Natl. Acad. Sci. USA* **2004**, *101*, 4089 – 4093.
[26] K. Inoue, H. Yamada, K. Akasaka, C. Herrmann, W. Kremer, T. Maurer, R. Döker, H. R. Kalbitzer, *Nat. Struct. Biol.* **2000**, *7*, 547 – 550.
[27] C. Antz, et al., *Nature* **1997**, *385*, 272 – 275.
[28] I. Rosnizeck, et al., *Angew. Chem.* **2010**, *122*, 3918 – 3922; *Angew. Chem. Int. Ed.* **2010**, *49*, 3830 – 3833.
[29] I. Rosnizeck, M. Spoerner, T. Harsch, S. Kreitner, D. Filchtinski, C. Herrmann, D. Engel, B. König, H. R. Kalbitzer, *Angew. Chem.* **2012**, *124*, 10799 – 10804; *Angew. Chem. Int. Ed.* **2012**, *51*, 10647 – 10651.

